Article citation info:
FLIZIKOWSKI J, TOPOLIŃSKI T, OPIELAK M, TOMPOROWSKI A, MROZIŃSKI A. Research and analysis of operating characteristics of energetic biomass micronizer. Eksploatacja i Niezawodnosc – Maintenance and Reliability 2015; 17 (1): 19–26.

Józef FLIZIKOWSKI
Tomasz TOPOLIŃSKI
Marek OPIELAK
Andrzej TOMPOROWSKI
Adam MROZIŃSKI

# RESEARCH AND ANALYSIS OF OPERATING CHARACTERISTICS OF ENERGETIC BIOMASS MICRONIZER

# BADANIA I ANALIZA EKSPLOATACYJNYCH CHARAKTERYSTYK MIKRONIZATORA ENERGETYCZNEJ BIOMASY*

*The analysis covers interrelations between the following factors: the machine movement, states and transformations of particles of the micronized biomass, particle shifts, mixing, grinding of energetic straw and its particles. It has been found that these relationships, among other things, depend on friction conditions, impacts, cutting, structural components of the micronizer as the dynamic movement of the machine structural components and biomass (particles) takes place under the conditions of idle movement and workload in order to accomplish an external goal. This paper aims at systematization, calculation and complementary research on micro-grinding performance characteristics (idle and operating), for constant and different rotational speeds (angular and linear).*

***Keywords:*** *operating characteristics, biomass, grinding.*

*Poddano analizie wzajemne relacje: ruchu użytkowego, stany i przemiany cząstek rozdrabnianej biomasy, ich przemieszczenia, mieszanie, rozdrabnianie słomy energetycznej i jej cząstek. Wykazano, że zależą one m.in. od warunków tarcia, zderzeń, cięcia, cech konstrukcyjnych mikronizatora, przy czym dynamiczne przemieszczanie elementów (części) konstrukcji maszyny i biomasy (cząstek), następuje w warunkach ruchu jałowego i obciążenia roboczego, dynamicznej realizacji celu zewnętrznego. Celem pracy jest systematyzacja, obliczenia i badania uzupełniające charakterystyk użytkowych (jałowych i roboczych) mikro-rozdrabniania, sporządzanych przy stałej i różnej prędkości obrotowej (kątowej lub liniowej).*

***Słowa kluczowe****: charakterystyki eksploatacyjne, biomasa, rozdrabnianie.*

## 1. Introduction

Both European and home regulations impose on electricity producers strict rules concerning energy production (according to fixed dates) requiring to generate more and more energy from renewable sources. By the year 2020 the percentage share of renewable sources in total energy consumption in Poland will have to be 15% (in the European Union 20%) and according to the Ministry of Economy of in 2010 this share was 9.5% (Polish Energy Policy – PER 2030. Polish agriculture is capable of providing sufficient amount of energetic plants (biomass) which properly processed will allow to decrease dependence of the Polish economy on fossil fuels. This will also enable to reduce emission of harmful products of combustion.

One of methods to be used for reduction of fossil fuels consumption is industrial co-combustion of biomass and coal. However, it poses some problems such as for example unburnt particles that are left both in slag and fly ash. Evidently, it is a loss of energy as the fuel does not deliver its whole energy and its unused part is irreversibly lost [3, 8, 21, 31].

The investigations carried out in power plants which burn biomass have revealed significant influence of the biomass fraction dimensions on the final content of coal in ash [3, 5, 6]. In order to prevent from this to happen it is necessary to apply a repeatable process of biomass grinding to achieve possibly the tiniest solid fractions.

The experiences of the Polish power plants indicate clearly that the outlays and costs connected with the process are high, depending on:

- decrease in energy efficiency of boilers which are subjected to the process of modernization and adjustment to perform biomass combustion, due to change in the way of heat exchange, especially the growing amount of unburnt matter,
- Increase in electrical energy demand by installation of a device for preparation and combustion of biomass (transport systems, precise milling etc.),
- significant increase in residue of furnace fireboxes impairing availability of boilers,
- fast corrosion due to high temperature caused by chlorine content in biomass (mainly straw),
- instability of biomass price on the free market caused by big competition and significant dispersion of the material providers [14].

Advantages of co-combustion include:

- lower emission of harmful compounds :$SO_2$, $NO_x$, $CO_2$,which has a positive influence on the environment and on the price of a generated heat unit (ETS)
- flexibility of the process – when there is not enough biomass the boiler can be used only for burning coal,
- co-combustion process is stabilized by burning coal [13, 15, 19].

(*) Tekst artykułu w polskiej wersji językowej dostępny w elektronicznym wydaniu kwartalnika na stronie ***www.ein.org.pl***

This study presents a description and analysis of technical conditions necessary for preparation of high quality product of biomass grinding (micronization) with the use of a micronizer as well as an analysis of its operating characteristics which will enable to develop of a new grinding technology for appropriate preparation of energy efficient biomass to be co-burnt with coal.

In order to achieve the goal, the following aspects have been studied: the nature of co-combustion, availability of biomass for energy production, development of a new technology of micro-grinding to optimize the process.

## 2. The nature of co-combustion technology

Co-combustion involves simultaneous burning of coal and biomass in a furnace firebox of a boiler thus distributing the heat into the system. Boilers (eg.OP-230) were designed to burn only coal, hence after being adjusted to co-combustion of biomass they are bound to reveal some decrease in heat output due to application of fuel with lower energy value [8, 11, 12, 15, 19, 22, 23].

Apart from the biomass heating value, its moisture is important for the combustion process as well [1]. Dry biomass burns very well with stable flame, whereas moist biomass moves the flame cone up the furnace firebox which is undesirable due to NOx emission and deterioration of heat exchange in boiler [8]. In order to obtain maximum economic efficiency it is necessary to produce ash with the content of combustible parts lower than 6% which can be sold to cement plants for production of e.g. cellular concrete [8].

## 3. Precision milling engineering

To prevent from numerous adverse phenomena connected with co-combustion of biomass and coal it is necessary to provide repeatable operating characteristics and precision milling of biomass to obtain most possible tiny solid fractions.

Capacity of the most commonly used hammer mills strictly depends on: the purpose of grinding, the mill structure, especially the working set(tools), quality parameters of the process, biomass quality, amount of ash and friction material contained in the material to be milled [11, 16, 20, 32]. In the lines available for preparation of furnace feed biomass is most frequently transported by worm conveyors and directed to hammer mills. Hammer mills can comminute the supplied biomass into dust with granulation degree up to 1mm [2,4,5,6]. In order to provide the comminuted biomass with appropriate quality/quantity, during operation at full capacity and in case of the machine shutdown or its overhaul, the systems are equipped with numerous mills (e.g. four sets of mills).

A micronizer (Fig. 1), along with the technological line (Fig. 3) [28], was applied to the Patent Office on 24.03.2011 under the title *Method and Device for Biomass Micronization* – no. P.394325.

The heart of a micronizer is fast rotating disk (17) driven by shaft (18), whose integral part are straight or arc blades. The disk can be opened or closed. Revolutions of the disk are matched so that it is possible to provide its external diameter with very high peripheral speed in the range (300–800) $m \cdot s^{-1}$.

High usable rotational speed of the disk causes generation of high sub-pressure in the zone of drying and initial grinding (24) in result of which the speed of air flowing onto the disk ranges between (250….350) m/s. Biomaterial is sucked by the flowing air which rapidly accelerates and hits the disk (17) in zone (24) undergoing initial grinding.

Under the influence of centrifugal forces the micronized material together with the air change the direction of flow from axial to perpendicular to working disk rotary axis (17).

After entering the channels between the blades it is then accelerated up to the value to match the disk diameter and its rotational speed.

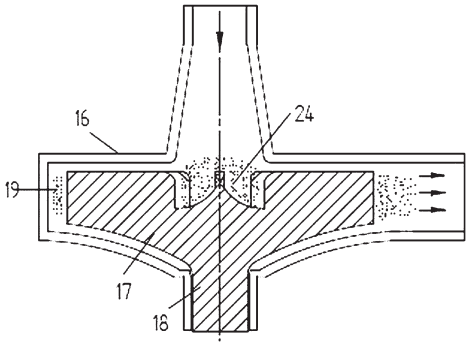


*Fig. 1. Device for biomass micronization according to patent application P. 394325; 16 – casing, 17 – rotational disk, 18 – drive shaft, 19 – high turbulence zone, 24 – initial micronization zone*

In effect of the physical factors impact the material is ejected to high turbulence zone (19) where it is micronized in the process made up of coexisting three processes: deagglomeration, densification and disintegration caused by cavitation and propagation of impact waves in result of radial-peripheral collisions of supersonic mass flows.

After filling the feed port (Fig. 1 and 2) the overlap of the process channel cross-sections starts to diminish. The initial assumption was that in each particle undergoes division in the micronization space (through friction, impacts, equalization of tensions). The assumption was made that the position of micronized particles in relation to the micronization plane is of random character and with uniform distribution. Thus, in effect of micronization, the particles with initial length disintegrate with similar probabilities, each into two smaller parts, each with the sum of lengths being the length (dimension) prior to division.

The very process of disintegration is caused by the state of complex loads /permanent strains and it always occurs in the material which, before being shifted, was in the preceding section of the working set (Fig. 2). Distribution of the particle length during grinding, in a material which has filled empty space of the (n+1) th segment, changes according to dependence [25, 26]:

$$\tilde{\rho}_{n+1}^{m}(x) = A_{n,m}\rho_n^m = \left(1 - \frac{x}{y_{n+1} - \tilde{y}_{n+1}^{m}}\right)\rho_n^m(x) + \frac{1}{y_{n+1} - \tilde{y}_{n+1}^{m}}\int_x^{l_{\max}} \rho_n^m(l)\,dl, \quad (1)$$

whereas, in a material which has been left in the n-th segment:

$$\tilde{\rho}_n^{m+1}(x) = \tilde{B}_{n,m}\rho_n^m = \left(1 - \frac{x}{\tilde{y}_n^m}\right)\rho_n^m(x) + \frac{1}{\tilde{y}_n^m}\int_x^{l_{\max}} \rho_n(l)\,dl, \quad (2)$$

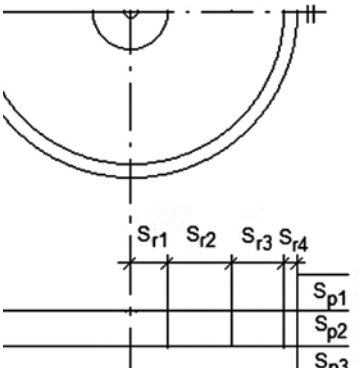


*Fig. 2. Radial segments of straw particle micronization: $S_{r1}/S_{P1}$ - initial introductory zone/level, $S_{r2}/S_{P2}$ - zone/level of initial acceleration of particles, Sr3/SP3 - working zone/level, Sr4/SP4 - zone/level of biomass particles impact division.*

The obtained functions are non-negative, being a sum of non-negative elements. By integrating, according to the product dimension, from 0 to *l*, it is easy to check that the functions are probability distributions:

$$\int_0^{l_{\max}} \tilde{\rho}_n^{m+1}(x)dx = 1 - \frac{\bar{x}}{\tilde{y}_n^m} + \frac{1}{\tilde{y}_n^m}\int_0^{l_{\max}}\int_x^{l_{\max}} \rho_n(l)dldx = 1 - \frac{\bar{x}}{\tilde{y}_n^m} + \frac{1}{\tilde{y}_n^m}\int_0^{l_{\max}}\int_0^{x} \rho_n(l)dxdl = 1 - \frac{\bar{x}}{\tilde{y}_n^m} + \frac{1}{\tilde{y}_n^m}\int_0^{l_{\max}} x\rho_n(l)dx = 1 \tag{3}$$

and similarly, for distribution $\tilde{\rho}_{n+1}^m$. Thus, operators $A_{n,m}$ and $\tilde{B}_{n,m}$ are correctly determined stochastic operators.

For simplification, it was assumed that after grinding the distribution of grain length in the (n+1)th segment will be homogenous (the comminuted fraction and the one present in the segment before division will get mixed), thus being a weighted mean from z $\rho_{n+1}^k$ i $\rho_n^k$:

$$\rho_{n+1}^m(x) = \frac{\tilde{y}_{n+1}^m}{y_{n+1}}\rho_{n+1}^{m-1} + \frac{y_n - \tilde{y}_{n+1}^m}{y_{n+1}} A_{n,m}\rho_n^m(x) \tag{4}$$

Removal process: After division, the layers (streams) of the micronized material move (are shifted) in relation to each other in the directions set by working channels of the revolving disk this generating centrifugal force and acceleration with a gradient of interacting speeds caused by mass differences of the biomass particular particles . The particles are removed from the preceding segment (it is affected by the component of centrifugal force induced by the shape model of working channels, a force whose direction is perpendicular to the working plane of a channel in which take place difficult to describe aerodynamic phenomena boosting the micronization process), whereas, they are not removed from the successive segment (as the component of force is perpendicular in the direction from the disk).

Thus, after division, the length distribution will be [27]:

$$\tilde{\rho}_n^{m+1}(x) = B_{n,m}\rho_{n,m} = \begin{cases} \tilde{\rho}_n^{m+1}(x)\left(\int_{l_{\min}}^{l_{\max}} \tilde{\rho}_n^{m+1}(x)\right)^{-1} & x \rangle l_{\max} \\ 0 & x \langle l_{\min} \end{cases} \tag{5}$$

The level of material after the *m-th* division (before *m*+1) in the *n*-th segment, $\tilde{y}_n^{m+1}$ is as follows:

$$\tilde{y}_n^{m+1} = \left(y_n - y_{n+1} + \tilde{y}_{n+1}^k\right)\left(1 - \frac{\int_0^{l_{\min}} \tilde{B}_{n,m}\rho_n^m(x)xdx}{\int_0^{l_{\max}} \tilde{B}_{n,m}\rho_n^m(x)xdx}\right) \tag{6}$$

In order to obtain distribution of the channel whole space before the *(m+1)-th* division (after being covered again), it is necessary to use a weighted mean:

$$\rho_n^{m+1}(x) = \frac{y_n - \tilde{y}_n^{m+1}}{y_n} A_{n-1,m}\rho_{n-1}^m + \frac{\tilde{y}_n^{m+1}}{y_n} B_{n,m}\rho_n^m \tag{7}$$

Operator $B_{n,m}$ is not linear like $A_{n,m}$, as it depends on the level of material which was left in the *n-th* segment after the first division and is a function of probability distribution in the material (which has an influence on which part of the material is to be removed from the disk and the division space). In order to be able to treat *Bn,m* as linear operators, quantities $y_n^m$ need to be treated in each step of the procedure, as being pre assigned and iteratively adjusted to experimental tests [17, 24].

The flow of particles leaving the machine. During the m-th micronization, the flow of particles leaving the machine through a gap between the n-th and the (n+1)th segments is given by the probability distribution:

$$s_n^m(x) = \begin{cases} \int_x^{l_{\max}} \rho_n(l)dl\left(\int_0^{l_{\min}}\int_x^{l_{\max}} \rho_n(l)dldx\right)^{-1} & l \langle l_{\min} \\ 0, & l \rangle l_{\min} \end{cases} \tag{8}$$

and its volume is equal to:

$$V_n^m(x) = \left(y_n - y_{n+1} + \tilde{y}_{n+1}^k\right)\frac{\int_0^{l_{\min}} \tilde{B}_{n,m}\rho_n^m(x)xdx}{\int_0^{l_{\max}} \tilde{B}_{n,m}\rho_n^m(x)xdx} \tag{9}$$

Linear velocity of grinding in the disk adjacent segments:

$$\begin{aligned} \Delta v_{L(i+1)-j/i-k} &= v_{(i+1)-j} - v_{i-k} \\ \Delta v_{L(i+1)-j/i-k} &= \pi \cdot D_{(i+1)-j} \cdot n_{i+1} - \pi \cdot D_{i-k} \cdot n_i \\ \Delta v_{L(i+1)-j/i-k} &= \pi \cdot (D_{(i+1)-j} \cdot n_{i+1} - D_{i-k} \cdot n_i) \end{aligned} \tag{10}$$

where:

$\Delta v_{L(i+1)-j/i-k}$ – gradient of linear velocity between adjacent ra dial segments ($S_{r1\text{-}4}$) or peripherals of the grinding set disk m·s$^{-1}$,

$v_{(i+1)-j}$ – linear velocity in the *(i+1) th* segment, on the *j-th* level ($S_{p1\text{-}4}$), m·s$^{-1}$,

$v_{i-k}$ – linear velocity in the *(i+1) th* segment, on the *k-th* level ($S_{p1\text{-}4}$), m·s$^{-1}$,

$D_{(i+1)-j}$, $D_{i-k}$ – respective guide diameters of the *(i+l)-th* segment (Sr1-4)and the *i-th* level ($S_{p1\text{-}4}$), *j-th* or the *k-th* row of grinding ($S_{r1\text{-}4}$), m,

$n_{i+1}$ – rotational speed of a segment more distant from the feed entry (e.g. Sr3), s$^{-1}$,

$n_i$ – rotational speed of a segment closer to the feed entry (e.g. Sr2), s-1;

Thus, it is necessary to match the working disk rotational (angular) speed in such a way that the speed of particles micronized in its particular segments would be of (sub)optimal range:

$$\omega = f(\Delta v_{L(i+1)-j/i-k}) \tag{11}$$

Transformations of particle length distributions. The distribution of particle lengths in the *n-th* division is expressed by denotation $\rho_n^m$. Operators which carry out distribution $\rho_n^m$ w $\rho_{n+1}^m$ i w $\rho_n^{m+1}$ are denoted respectively as $A_{n,m}$ i $B_{n,m}$.

State $\rho_0^0$ is given (distribution of particle lengths in the input material, e.g. the first grinding, second grinding ,…..). State $\rho_n^m$ is obtained from an equation of the sum of A and B operator products in state $\rho_0^0$. The products represent all the paths which can be used to reach this state from state $\rho_0^0$. For example:

$$\rho_2^3 = \left(A_{1,2}A_{0,1}B_{0,0} + A_{1,2}B_{1,1}A_{0,0} + B_{2,2}A_{1,1}A_{0.0}\right)\rho_0^0 \tag{12}$$

State $\rho_n^m$ can be reached by using operator A n times and operator B² m-times. The path is unambiguously defined by an n-element subset of steps making up the whole path { 1……m}, steps with operation of operator A. The number of such subsets, that is, products in the sum is $\binom{m}{n}$. In general, operators A and B do not commute. Calculation of such expressions is crucial for further studies. States $\rho$ are positive elements of Banach space $L^1$ ([0, 1]), whereas operators *A* and *B* are endomorphisms of this space [9, 29, 30]. For practical reasons it is necessary to approximate *p* states by positive elements $R^d$, and operators *A* and *B* by matrixes *d*×*d*. Physically, it corresponds to division of a particle of length l (e.g. the feed initial dimension) into d-number of further indivisible parts (e.g. product dimension close to 0) – corresponding to a linear measure of disintegration (degree). It can also correspond to dimensional classes: (l>1.4) mm, (0.8<l<1.4) mm, (0.4<l<0.8) mm, (l<0.4) mm.

Literature offers inconsistent data on the amount of straw to be used for energy production purposes. However, it can also be accepted that the surplus between its total production and utilization in agriculture in 2010 was 11.6 mln tons [Flizikowski 2011, Flizikowski 2013].

Fig. 3 shows a scheme of a technological system for biomass grinding. The micronized material is supplied through a dumping hopper, to basket (1) from where it is delivered by conveyor (2) to feeder (3). The feeder fills a suction pipe which feeds an axial-disk micronizer powered by an electric motor (4). The micronized biomass flows in the form of air and vapor mixture to cyclone separator (5), from where it is fed to external containers by conveyor belt (6). Humid air free from micronized material flows to a drier and next to fine filter (7), from where it is carried outside. Fractions separated from both filters are turned to a second micronization (thick fraction) or are supplied to external containers (fine fraction). Dust silos, bag filters and biomass silos are equipped with anti-explosion systems [7, 8, 23].

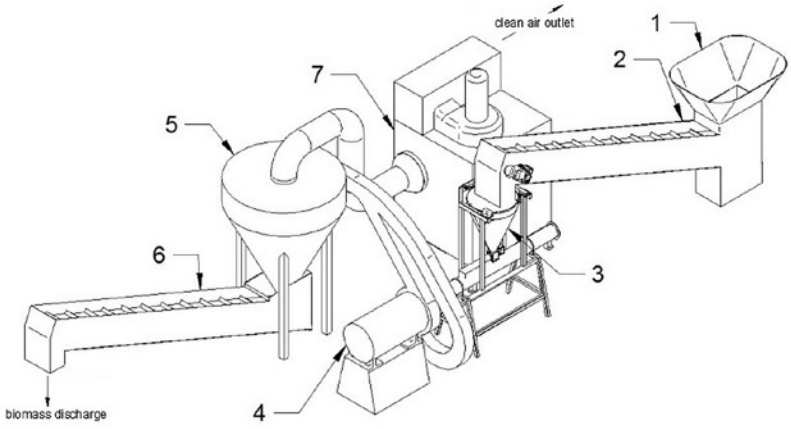


*Fig. 3. Technological system for biomass micronization: 1-basket with dumping hopper, 2-coveyor belt, 3-feeder, 4-micronizer with electric motor, 5-cyclon, 6-conveyor belt,7-filtration device*

## 4. Presentation of micronization experiments results (Statistica 10)

The tests were carried out on a test stand, being a prototype innovative technological system for biomass micronization.

A comparison of measuring elements: mass and percentage share of the investigated rye straw fractions has been presented in table1 for selected rotational speeds of the first micro-milling.

A sample of rye straw was the statistical population. The tests involved a quantitative feature, that is, the share of mass of particular

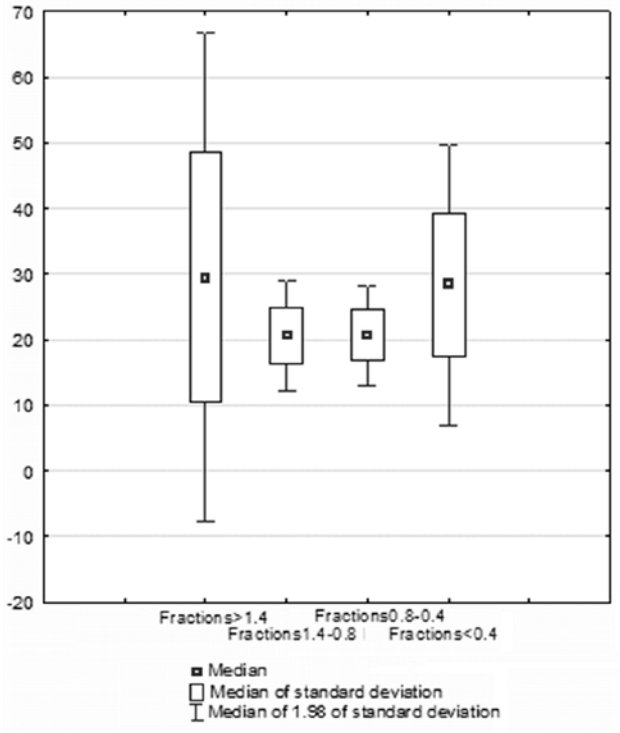


*Fig. 4. Values of the mean and percentage mass content of the tested fractions for range rotational speed range (0…18.000) min$^{-1}$ in testing time of 10s*

fractions in the sample total mass, measured in % in relation to the value of rotational speed in two time intervals (10 and 30) s. A portion of rye straw with mass 40 g served as a statistical unit, 12 such portions were tested. Four kinds of fractions were separated: (> 1.4, 1.4–0.8, 0.8–0.4 and < 0.4)mm and eleven values of rotational speed – (from 0 to 18.000) min$^{-1}$.

Statistical measures are used for a description of the tested specimen structure (Tab. 1).

The mean percentage share of rye straw fraction (>1.4) mm of the micronization product was 29.52%, for all the rotational speeds, in time of 10 seconds, fraction (1.4–0.8) mm – 20.563%, fraction (0.8–0.4) mm – 20.683%, and fraction (< 0.4) mm – 28.319%. It means that the highest mean percentage was found for the extreme intervals. Half of specimens of fraction (>1,4) mm contained 27.488%, fraction (1.4–0.8) mm and (0.8-0.4) mm – nearly 21.5 %, and fraction (< 0.4) mm – 28.087% (median).

In the studied population, there occurs relation Xśr>Me between the measures of central tendency in fractions (>1.4) mm and (<0.4)mm which indicates right sided asymmetry (not dangerous) and in fractions (1.4–0.8) mm and (0.8–0.4) mm – relation Xśr< Me, (<0.4) mm – 6.203% (feed), which indicates left sided asymmetry (not dangerous, either). The lowest percentage share of rye straw fraction for all rotational speeds, during 10 seconds, was found for fraction (<0.4) mm – 6.203% (feed), and the highest for fraction (>1.4) mm – 74.240% (feed). The highest absolute difference between value of the highest and the lowest percentage share was: in fraction (<0.4) mm – 6.203% (feed), and the highest in fraction (>1.4) mm – 62.946, and in fraction (<0.4) mm – 35.726. The lowest value of range was observed in fraction (0.8–0.4) mm – 13.995. Portions of rye straw dust were characterized by diversified mass percentage share of particular fractions.

On the average it was ±18.989 % for fraction (<0.4) mm. The lowest value of standard deviation was found for fraction (0.8–0.4) mm –

*Table 1. Mass and percentage share of the tested rye straw fractions for selected rotational speeds.*

| Rotational speed $min^{-1}$, t=10s | Moisture of specimens , % | Mass of specimen, g | fraction > 1.4 | | fraction 1.4-0.8 | | fraction 0.8-0.4 | | fraction < 0.4 | |
|---|---|---|---|---|---|---|---|---|---|---|
| | | | mass g | share% | mass g | share % | mass g | share % | mass g | Share % |
| 0 (wsad) | 13.2 | 40.14 | 29.8 | 74.240 | 3.79 | 9.442 | 4.41 | 10.987 | 2.49 | 6.203 |
| 9000 | 13.0 | 40.1 | 16.32 | 40.698 | 7.71 | 19.227 | 7.17 | 17.880 | 8.51 | 21.222 |
| 10000 | 13.1 | 40.12 | 15.64 | 38.983 | 7.55 | 18.819 | 7.84 | 19.541 | 8.11 | 20.214 |
| 11000 | 13.2 | 40.04 | 15.93 | 39.785 | 7.41 | 18.506 | 7.73 | 19.306 | 8.5 | 21.229 |
| 12000 | 12.9 | 39.99 | 13.92 | 34.809 | 8.07 | 20.180 | 8.51 | 21.280 | 9.5 | 23.756 |
| 13000 | 13.0 | 40.09 | 11.02 | 27.488 | 8.65 | 21.576 | 8.7 | 21.701 | 11.26 | 28.087 |
| 14000 | 13.1 | 39.98 | 5.75 | 14.382 | 9.06 | 22.661 | 8.75 | 21.886 | 16.07 | 40.195 |
| 15000 | 12.9 | 40.02 | 4.52 | 11.294 | 9.28 | 23.188 | 9.16 | 22.889 | 16.78 | 41.929 |
| 16000 | 13.0 | 40.03 | 5.4 | 13.490 | 9.65 | 24.107 | 9.14 | 22.833 | 14.71 | 36.747 |
| 17000 | 13.2 | 40.15 | 6.17 | 15.367 | 9.84 | 24.508 | 9.73 | 24.234 | 14.18 | 35.318 |
| 18000 | 13.1 | 39.99 | 5.67 | 14.179 | 9,59 | 23.981 | 9.99 | 24.981 | 14.64 | 36.609 |
| 18000 t=30s | 13.0 | 40.07 | 5.25 | 13.102 | 9.87 | 24.632 | 9.08 | 22.660 | 15.54 | 38.782 |

*Table 2. Descriptive statistics of mass percentage share of the tested rye straw fractions for rotational speeds from 0 to 18.000 for testing time 10sec.*

| Variable | Mean | Median | Minimum | Maximum | Lower quartile | Upper quartile | Range |
|---|---|---|---|---|---|---|---|
| fraction > 1.4 | 29.520 | 27.488 | 11.294 | 74.240 | 14.179 | 39.785 | 62.946 |
| fraction 1.4-0.8 | 20.563 | 21.576 | 9.442 | 24.508 | 18.819 | 23.981 | 15.066 |
| fraction 0.8-0.4 | 20.683 | 21.701 | 10.987 | 24.981 | 19.306 | 22.889 | 13.995 |
| fraction < 0.4 | 28.319 | 28.087 | 6.203 | 41.929 | 21.222 | 36.747 | 35.726 |
| Variable | Variance | Standard deviation | Confidence limit Standard deviation – 95.00% | Confidence limit Standard deviation . +95.00% | Variabiity coefficient | Data skew | Curtosis |
| fraction > 1.4 | 360.58 | 18.989 | 13,268 | 33.324 | 64.327 | 1,300 | 1.9806 |
| fraction 1.4-0.8 | 18.50 | 4.301 | 3.005 | 7.548 | 20.917 | -1.870 | 4.3669 |
| Fraction 0.8-0.4 | 14.85 | 3.853 | 2.692 | 6.763 | 18,630 | -1.688 | 3.6968 |
| Fraction < 0.4 | 119.13 | 10.915 | 7.626 | 19.155 | 38.542 | -0.606 | -0.0923 |

3.853%. This dispersion is considered to be significant as the relative measure of variability (v) is maximally 64.327 % for fraction (>1.4) mm, and minimally 18.63% for fraction (0.8–0.4) mm (Tab. 2).

The highest diversity of the fraction mass percentage share for different values of rotational speed (from 0 do 18.000) $min^{-1}$, in testing time 10 seconds, was characteristic of fraction (>1.4) mm (range from 10.513 do 48.509) and fraction (<0.4) mm (from 17.404 do 39.234). The lowest diversity characterizes fractions (1.4–0.8) mm and (0.8–0.4) mm (from about 16.5 to app. 24.5) (Fig. 4).

The results of Shapiro-Wilk test for rye straw dust fraction (>1.4) mm, for rotational speeds in the range (0…18.000) $min^{-1}$ and testing time 10 seconds, indicate its distribution normality (W=0.083708, p=0.02892). For the analyzed fraction, the lower quartile is equal to 14.179%, which means that 25% of all the obtained results was below this value. The upper quartile is equal to 39,785%, hence 25% of all the results is found to be above this value.

The results of Shapiro-Wilk test for rye straw dust fraction (1.4–0.8) mm for rotational speed in the range (0...18.000)$min^{-1}$ and testing time 10 seconds, indicate its normal distribution (W=0.80469, p=0.01084). The lower quartile for this fraction is equal to 18,819%, and the upper one is 23.918%.

The results of Shapiro-Wilk test for rye straw dust fraction (0.8-0.4) mm for rotational speed in the range (0…18.000)$min^{-1}$ and testing time 10 seconds, indicate its normal distribution. (W=0.85496, p=0.04953). The lower quartile for this fraction is equal to 19.306%, and the upper one is 22.889%.

The results of Shapiro-Wilk test for rye straw dust fraction (<0.4) mm, for rotational speeds in the range ((0…18.000) $min^{-1}$ and testing time 10 seconds, indicate lack of its distribution normality (W=0.92245, p=0.33961). For the analyzed fraction the lower quartile is equal to 21.222%, and the upper one is 36.747%.

The value percentage share of rye straw dust fraction (>1.4) mm is strongly negatively correlated with the rotational speed increase in the range (0…18.000)$min^{-1}$ (r=−0.96) which means that the percentage share of fraction (>1.4) mm in the whole sample mass decreases along with an increase in rotational speed (Fig. 5). This dependence is described by regression equation:

$$fraction > 1.4 = 74.682 - 0.0037 \cdot \omega$$

The value percentage share of rye straw dust fraction (1.4–0.8) mm is strongly positively correlated with rotational speed increase in

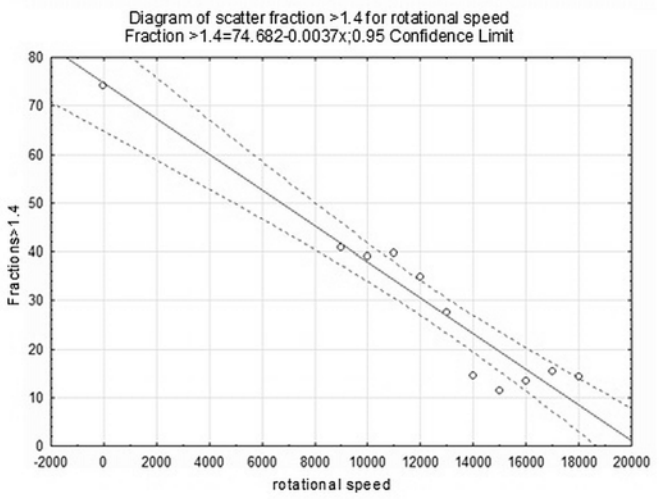


*Fig. 5. Diagram of scatter for rye straw dust fraction (>1.4) mm for rotational speed of the range (0…18.000)min$^{-1}$ and testing time 10 s.*

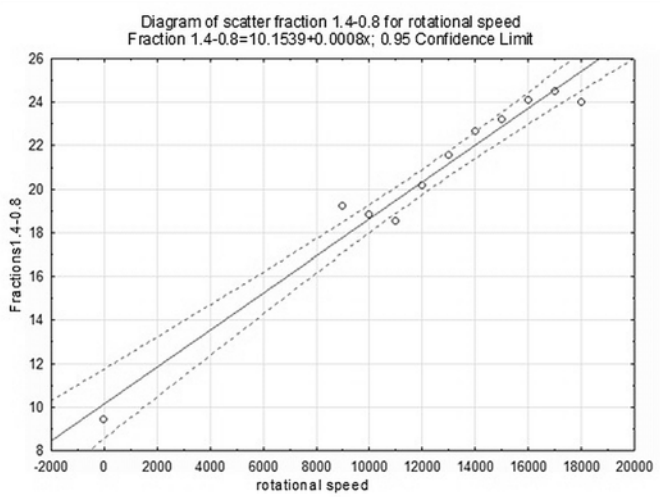


*Fig. 6. Diagram of scatter for rye straw dust fraction (1.4–0.8) mm for rotational speed of the range (0…18.000)min$^{-1}$ and testing time 10 s.*

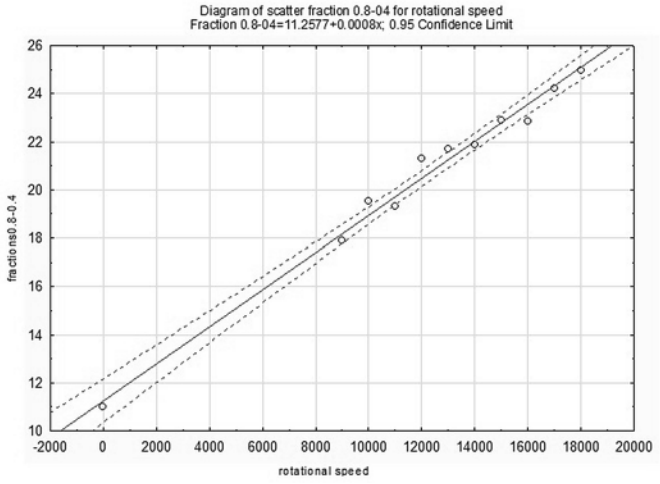


*Fig. 7. Diagram of scatter for rye straw dust fraction (0.8–0.4) mm for rotational speed range (0…18.000)min$^{-1}$ and testing time 10*

the range (0…18.000)min$^{-1}$(r=−0.98) which means that the share of fraction (1.4–0.8) mm in the whole sample mass increases along with an increase in rotational speed (Fig. 6). This dependence is described by regression equation:

$$fraction\ 1.4\text{-}0.8 = 10.1539 + 0.0008 \cdot \omega$$

The value percentage share of rye straw dust fraction (0.8–0.4) mm is strongly positively correlated with rotational speed increase in the range (0…18.000)min$^{-1}$ (r=−0.99) which means that the share of fraction (0.8–0.4) mm in the whole sample mass increases along with an increase in rotational speed (Fig. 7). This dependence is described by regression equation:

$$fraction\ 0.8\text{-}0.4 = 11.2577 + 0.0008 \cdot \omega$$

The value percentage share of rye straw dust fraction (<0.4) ) mm is strongly positively correlated with rotational speed increase in the range (0…18.000)min$^{-1}$ (r=−0.90) which means that the share of fraction (<0.4) mm in the whole sample mass increases along with an increase in rotational speed (Fig. 7). This dependence is described by regression equation:

$$fraction < 0.4 = 3{,}951 + 0.002 \cdot \omega$$

Also a comparative analysis of changes in mass percentage share of particular fractions has been performed through multiple grinding and for constant rotational speed 18.000min$^{-1}$, for different testing times (10 and 30) s (Tab. 5). The obtained data shows that the percentage share of fraction (>0.8–0.4) mm decreases along with the process duration and the percentage share of fraction (0.25–0.4) mm increases, especially dusts (<0.25) mm (Tab. 5, Fig. 8).

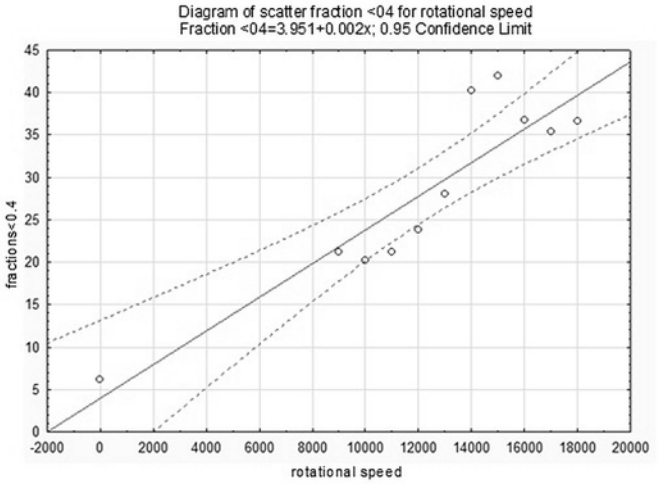


*Fig. 8. Diagram of scatter for rye straw dust fraction (< 0.4) mm for rotational speed in the range (0…18.000)min$^{-1}$ and testing time 10 seconds.*

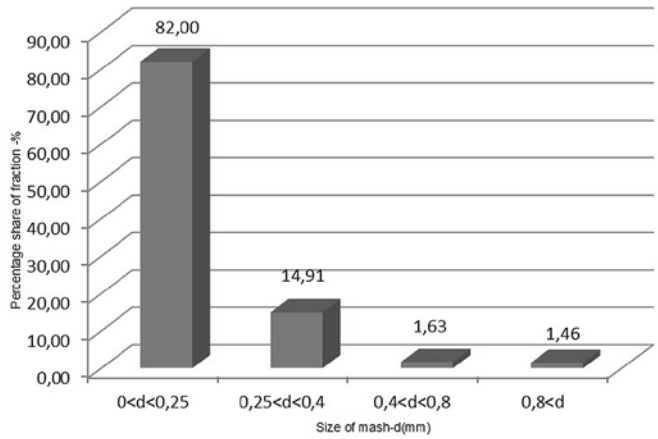


*Fig. 9. Grain distribution for Specimen 2*

*Table 3. Mass and percentage shares of dimensional fractions from the analysis of Specimen no.2, (the second micro-milling)*

| Size of sieve mesh d (mm) | Mass of fraction $m_1$ (g) | Mass of fraction $m_2$ (g) | Mass of fraction $m_3$ (g) | Mean mass $m_{śr}$ (g) | Percent % |
|---|---|---|---|---|---|
| 0<d<0,25 | 32.95 | 32.48 | 32.97 | 32.80 | 82.00 |
| 0,25<d<0,4 | 5.98 | 5.95 | 5.96 | 5.96 | 14.91 |
| 0,4<d<0,8 | 0.62 | 0.82 | 0.52 | 0.65 | 1.63 |
| 0,8<d | 0.45 | 0.75 | 0.55 | 0.58 | 1.46 |

## 6. Conclusions

The carried out tests and analysis have proved that application of a micronizer in the process of preparation of biomass to be co-combusted with coal provides numerous benefits. Besides, thanks to the tests the influence of operating characteristics of the micronizer on the process quality improvement has been defined.

In the first micro-milling of straw particles the percentage share of rye straw dust highest fraction (>1.4) mm is strongly negatively correlated with an increase in rotational speed in the range (9.000… 18.000) $min^{-1}$ (r=−0.96). This means that the percentage share of fraction (>1.4) mm in the product entire mass increases along with an increase in angular velocity (experimentally by 28%).

Whereas, the percentage share of rye straw dust fraction (1.4–0.8) mm is strongly positively correlated with angular velocity increase in the range (9.000…18.000)$min^{-1}$ (r=0,98) which means that the share of fraction (1.4–0.8) mm in the entire sample mass increases along with an increase in angular velocity

The share of the smallest fraction value (<0.4) mm of rye straw dust is strongly positively correlated with rotational speed increase in the scope of (9.000…18.000)$min^{-1}$(r=0.90). The share of fraction (<0.4) mm in the total mass of the sample increases along with rotational speed (in experimental range even by 21%). The second micro-milling of the product provides satisfactory qualitative results: totally nearly 96% of the tiniest fraction (<0.40) mm.

Along with an increase in rotational speed the percentage share of fraction (<0.4) mm in the whole mass of the specimen increases ( experimentally even by 21%). The second micro-milling of the product provides satisfactory qualitative results: totally app. 96% of the tiniest fraction (<0.40) mm.

The above mentioned advantages of biomass make it a desirable material for energy production and it seems that the Polish power generation industry is bound to develop biomass micro-grinding for energy generation. Political conditionings (both internal and European) impose strict rules on power producers involving respecting the requirements concerning the use of renewable sources for energy production according to strictly fixed dates. Agricultural character of Polish economy provides good conditions for farming energy providing plants which can limit the dependence on fossil fuels.

On the basis of the micro-grinding tests results it can be said that along with an increase in the process duration time the percentage share of fraction (>0.8–0.4) mm decreases and the percentage share of energetically desired fractions increases: (0.25–0.4) mm, especially dusts (<0.25) mm.

*The research was performed in the company Hydrapress Sp. z o.o. within the project POIG 01.04.00-04-003/11-00: "Improvement of competitiveness of the company through the development of biomass shredding technology"*

## References

1. Armstrong P R, Lingenfelser J E, McKinney L. The Effect of Moisture Content on Determining Corn Hardness form Grinding Time, Grinding Energy, and Near – Infrared Spectroscopy. Applied Engineering in Agriculture 2007; 23(6): 793-799.
2. Bieliński K S, Flizikowski J B. Sterowanie rozgrywające i rozliczanie energomediów w obiektach. EKOMILTARIS, WAT, Zakopane 2008.
3. Błasiak W, Moberg G, Grimbrandt J. Redukcja tlenków azotu oraz optymalizacja spalania w komorach kotłów za pomocą asymetrycznego systemu podawania powietrza wtórnego. 10 Międzynarodowa Konferencja Technik Grzewczych, Göteborg, 2006.
4. Flizikowski J. Inteligentny system rozdrabniania. Inżynieria i Aparatura Chemiczna 2011; 3(50): 22-24.
5. Flizikowski J. Poziomy inteligentnego systemu rozdrabniania. Inżynieria i Aparatura Chemiczna 2011; 3(50): 24-26.
6. Flizikowski J. Micro - and Nano – energy grinding. Panstanford Publishing, Singapore, 2011.
7. Głód K, Rysiawa K. Współspalanie biomasy. Instytut Chemicznej Przeróbki Węgla. XV Wiosenne Spotkanie Ciepłowników. Zakopane 2008.
8. Golec T. Współspalanie biomasy w kotłach energetycznych. Energetyka 2004; 7(8): 437-445.
9. Hoffman P C, Ngonyamo-Majee D, Shaver R D. Technical note: Determination of can hardness in diverse corn gin diverse corn germplasm using near-infrared reflectance baseline shift as a measure of grinding resistance. Journal of Dairy Science 2010; 93(4): 1685-1689.
10. Kowalik K, Sykut B, Marczak H, Opielak M. A method of evaluating energy consumption of the cutting process based on the example of hard cheese. Eksploatacja i Niezawodnosc – Maintenance and Reliability 2013;15(3): 241-245.
11. Kruczek M, Skrzypczak G, Muraszkowski R. Spalanie i współspalanie biomasy z paliwami kopalnymi. Czysta Energia 2007; 68(6): 32-35.
12. Kryszak J. Wykorzystywanie biomasy dla pozyskiwania energii odnawialnej. Akademia Rolnicza, Poznań, 2005.
13. Kubica K. Spalanie biomasy i jej współspalanie z węglem. Instytut Chemicznej Przeróbki Węgla, Zabrze, 2004.
14. Laurow Z. Ekologiczne uwarunkowania pozyskiwania biomasy cele energetyczne w leśnictwie. Możliwości wykorzystania biomasy na cele energetyczne. Malinówka, 2003.
15. Lorenz U. Gospodarka węglem kamiennym energetycznym. IGSMiE, PAN, Kraków, 2010.
16. Macko M. Economic-energetic analysis of multi-edge comminution of polymer recyclates. Analiza ekonomiczno-energetyczna wielokrawędziowego rozdrabniania recyklatów polimerowych. Przem. Chem. 2013; 213(8): 1499-1502.
17. Mazurkiewicz D. A knowledge base of the functional properties of the conveyor belt adhesive joint for FEM simulation of its stress and strain state. Journal of Adhesion Science and Technology 2012; 26(10-11): 1429-1442.
18. Niederliński S. System i sterowanie. PWN, Warszawa, 1987.

19. Popiel P. Wpływ współspalania biomasy z pyłem węglowym na stratę niedopału. Prace Instytutu Elektrotechniki, Zeszyt 249, Politechnika Lubelska, 2011.
20. Powierża L. Zarys inżynierii systemów bioagro-technicznych. Wydawnictwo ITE, Radom, 1997.
21. Semczuk M. Ustawa o efektywności energetycznej - narzędzie w procesie budowy niskoemisyjnej i konkurencyjnej gospodarki. Rynek Energii I(V). Zeszyt tematyczny. Wydawnictwo KAPRINT, Lublin, 2010.
22. Soliński I, Jesionek J. Efekty ekologiczne współspalania biomasy z węglem kamiennym. Warsztaty; Współspalanie biomasy i termiczna utylizacja odpadów w energetyce. Kraków, 2007.
23. Ściążko M, Zuwała J, Pronobis M. Zalety i wady współspalania biomasy w kotłach energetycznych na tle doświadczeń eksploatacyjnych pierwszego roku współspalania biomasy na skalę przemysłową, Energetyka i Ekologia 2006; 3: 207-220.
24. Sharma B, Jones C L, Khanchi A. Tensile Strength and Shear Strength of Switchgrass Before and After Frost. Biological Engineering Transactions 2011; 4(1): 43-54.
25. Tomporowski A, Flizikowski J. Charakterystyki ruchowe wielotarczowego rozdrabniacza ziaren biomasy. Przem. Chem. 2013; 92(4): 498-503.
26. Tomporowski A. Stream of efficiency of rice grains multi-disc grinding. Eksploatacja i Niezawodnosc – Maintenance and Reliability 2012; 14(2): 150-153.
27. Tomporowski A, Opielak M. Structural features versus multi-hole grinding efficiency. Eksploatacja i Niezawodnosc – Maintenance and Reliability 2012; 14(3): 223-228.
28. Topoliński T. Flizikowski J. Jasiński J. Wełnowski D. Inżynieria energomechaniczna biomasy. Cz. II. Mikronizator. Inż. i Ap. Chem. 2013; 52(1): 9-10.
29. Vishwakarma R K, Shivhare U S, Nanda S K. Physical properties of guar seeds. Food Bioprocess Technology, 2012; 5: 1364-1371.
30. Walton O. Effects of interparticle friction and particle shape on dynamic angles of repose via particle - dynamics simulation. Proc. Conf. Mechanics and Statistical Physics of Particulate Materials, June 8-10, La Jolla CA, USA, 1994.
31. Węglarz A. Prawne aspekty efektywności energetycznej w Polsce w świetle Dyrektyw Unii Europejskiej. KAPE, Warszawa, 2010.
32. Zawada J, (red). Wprowadzenie do mechaniki maszynowych procesów kruszenia. ITE. Radom-Warszawa, 2005.

**Józef FLIZIKOWSKI**
**Tomasz TOPOLIŃSKI**
**Andrzej TOMPOROWSKI**
**Adam MROZIŃSKI**
Faculty of Mechanical Engineering
University of Technology and Life Sciences
ul. S. Kaliskiego 7., 85-789 Bydgoszcz, Poland
E-mails: fliz@utp.edu.pl, topol@utp.edu.pl,
a.tomporowski@utp.edu.pl, adammroz@utp.edu.pl
**Marek OPIELAK**
Department of Mechanical Engineering
Lublin University of Technology
Nadbystrzycka str.38, 20-816 Lublin, Poland
E-mail: m.opielak@pollub.pl